

Advantages of mixed unitary operators for quantum information processing

Anthony M. Polloreno*
Rigetti Computing, Berkeley, CA

Kevin C. Young
Sandia National Laboratories, Livermore, CA
(Dated: January 9, 2019)

Coherent errors in quantum operations are ubiquitous. Whether arising from spurious environmental couplings or errors in control fields, such errors can accumulate rapidly and degrade the performance of a quantum circuit significantly more than an average gate fidelity may indicate. As Hastings and Campbell have recently shown, randomly sampling an ensemble of implementations of a target gate yields an effective quantum channel that well-approximates the target, but with dramatically suppressed coherent error. Our results extend those of Hastings and Campbell to include robustness to drifting external control parameters. We implement these constructions using a superconducting qubit and will discuss randomized benchmarking results consistent with a marked reduction in coherent error.

I. INTRODUCTION

The past decade has seen a dramatic increase in the performance and scale of quantum information processors (QIPs). Gate fidelities are now routinely in the 99% to 99.99% range [1, 2], and dozens of individually-addressable qubits are becoming available on integrated devices. While these advances represent important steps forward on the path towards a computationally useful QIP, the quantum advantage milestone [3] has yet to be definitively reached. The limiting factor, of course, is errors in the quantum gate operations.

The impact of an error in a quantum gate depends strongly on both the magnitude and the nature of the errors. Systematic, or *coherent*, errors can arise from poorly calibrated controls or imperfect gate compilations that induce repeatable, undesired unitary errors on the state of a QIP. Errors of this type are correlated in time and add up coherently. They are computationally expensive to model and it is difficult to place tight analytic bounds on circuit performance. Contrast this against random, or *stochastic*, errors, which result from high-frequency noise in the controls or the environment. Systems with stochastic errors can be modeled by defining a rate of various discrete errors in the system, such as a bit flips or phase flips. These errors are significantly easier to simulate on a classical computer, and their impact on quantum circuits is much easier to estimate.

Despite the relative ease of modeling stochastic errors, coherent errors are often much more likely to appear in QIPs. While these errors can often be reconstructed using various tomographic techniques, their impact is difficult to predict. The diamond distance can be used to bound the total variation distance (TVD) of a quantum circuit, but it is in general sensitive at first order to repeated application of a gate with coherent errors. For

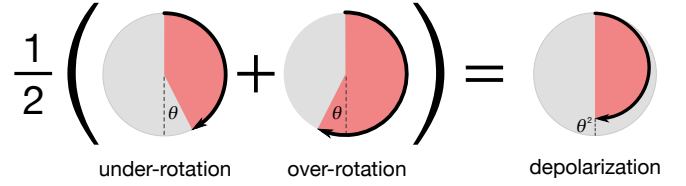


FIG. 1. An example of a mixed unitary process. Using optimal control, two implementations of a Z_π gate are designed to have equal and opposite sensitivity to errors (if one implementation over-rotates by angle θ , then the other *under*-rotates by θ). Each time the gate is used, one of these implementations is chosen at random. The resulting quantum channel is equivalent to a perfect implementation of the gate followed by dephasing of $\mathcal{O}(\theta^2)$.

long circuits, this can add up extremely quickly. Recent work by Campbell and Hastings[4–6], however, has shown that coherent noise can be strongly suppressed by probabilistically mixing several distinct implementations of the target quantum gates. The resulting effective quantum process has a diamond distance that grows only quadratically in the over/under rotation angle of the component gates.

In this article we discuss various applications of these mixed unitary controls, and show that the advantages of this approach can be made robust to drift in the gate implementations. We demonstrate that, depending on the objective, different numerical optimizations may be preferred. We present an experimental implementation of single-qubit mixed unitary controls on a superconducting qubit testbed at Rigetti Computing. Using randomized benchmarking, we are able to show a marked improvement in error rates, as well as a reduced variance in circuit outcome probabilities, indicating a reduction in the coherence of the error. We further provide an optimal control approach to the mixed unitary control design problem, and apply our methods in simulation where we construct single- and two-qubit mixed unitary controls

* Email: anthony@rigetti.com

which are robust to drift and uncertainty in the control parameters.

II. MATHEMATICAL PRELIMINARIES

Quantum gate operations are implemented by applying a sequence of classical control fields to some set of qubits. Fluctuations in the environment or imperfections in the controls can cause the state of the qubits to change in a way that is different from what was intended. But if the gates are fairly stable with time and context[7], then we can usually describe their action on the qubit state using *process matrices* – linear, Markovian maps on the state of some qubits. When working with process matrices, it is convenient to write the system density operator using a vectorized representation, and in this article, we'll make use of the generalized Bloch vector,

$$\vec{\rho} = \text{Tr}(\rho \vec{\Sigma}), \quad (1)$$

where $\vec{\Sigma}$ is a vector of all 4^n n -qubit Pauli operators. The action of a gate is then given by the usual matrix multiplication:

$$\vec{\rho} \rightarrow \mathcal{G}\vec{\rho} = \mathcal{E}\tilde{\mathcal{G}}\vec{\rho}. \quad (2)$$

Here \mathcal{G} is the target operation, $\tilde{\mathcal{G}}$ is the actual gate as implemented, and \mathcal{E} is the effective error channel:

$$\mathcal{E} = \left(\begin{array}{c|c} 1 & \vec{0}^T \\ \hline \vec{m} & R \end{array} \right) \quad (3)$$

The top row of all trace-preserving (TP) maps is fixed to $\{1, 0, 0, 0, \dots\}$. The rest of the first column, \vec{m} , describes any deviations from unitality, as could arise from amplitude damping. If the error channel is unitary, then the error is coherent, and the submatrix R is perfectly anti-symmetric, corresponding to a rotation of the generalized Bloch vector. If R is diagonal, then the error channel is Pauli stochastic, with each entry corresponding to the probability that the associated Pauli error occurs in each application of the gate. Any such Pauli error is expressible as a unitary matrix U that acts on the density matrix by conjugation, and has an action on the vectorized density matrix given by:

$$\vec{\rho} \rightarrow \rho_i \vec{\Sigma}_{ijk} U_{kl}^\dagger \vec{\Sigma}_{lmn} U_{mj} \quad (4)$$

If R is symmetric but not diagonal, then the channel is still stochastic, but the random errors consist of correlated Pauli operators (such as $X + Y$). For a single qubit, this describes everything, but the situation can be slightly more complicated for more qubits.

In general, if we have a collection of single qubit controls $\{U_i\}$ generated by $\{H_i\}$, the channel that results

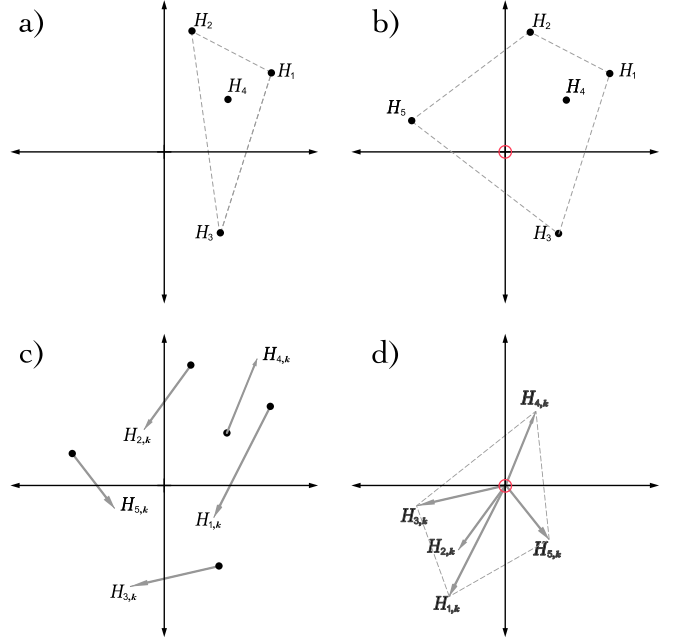


FIG. 2. A target unitary gate can be implemented a number of ways, each with a different effective Hamiltonian error. These error Hamiltonians lie in a vector space. a) Four effective Hamiltonians. The origin is not contained in their convex hull, so there are no 0MUPs. b) The origin is contained in the convex hull after adding an additional control solution. Because there are more than $n + 1$ implementations, there exist an infinite number of 0MUPs. c) The error Hamiltonians shown with their derivative with respect to a control parameter. As this parameter drifts, a 0MUP may drift, leading to a first-order error. d) The derivatives also lie in a vector space. If the origin lies in their convex hull, then it may be possible to construct a 1MUP.

from drawing from the controls probabilistically has elements given by:

$$\mathcal{M}_{jk} = \sum_i p_i \text{Tr}(\sigma_j^\dagger U \sigma_k U^\dagger) \quad (5)$$

$$= \sum_i p_i \text{Tr}(\sigma_j^\dagger \exp(i \frac{\theta_i}{2} H_i) \sigma_k \exp(-i \frac{\theta_i}{2} H_i)) \quad (6)$$

$$= \text{Tr}(\sum_i p_i (\sigma_j^\dagger \sigma_k \cos \theta_i^2 + \sigma_j^\dagger H_i \sigma_k H_i \sin \theta_i^2 + i \sigma_j^\dagger H_i \sigma_k \sin \theta_i \cos \theta_i - i \sigma_j^\dagger \sigma_k H_i \sin \theta_i \cos \theta_i)) \quad (7)$$

$$(8)$$

The first term corresponds to the identity, and $\sin \theta_i^2$ is always positive, so we cannot hope to eliminate the second term, but $\sin \theta_i \cos \theta_i$ may be positive or negative, and so there is hope that we could possibly combine various implementations to eliminate this term. The result would be a purely stochastic channel.

The problem of minimizing the last term:

$$\sum_i \sin \theta_i \cos \theta_i (\sigma_j^\dagger H_i \sigma_k - \sigma_j^\dagger \sigma_k H_i) \quad (9)$$

can equivalently be cast as trying to construct a family of vectors whose convex hull contains the origin. This can be seen in Figure 2 a) and b).

In addition to the type of errors, we care about the size of an error. The *size* of an error in quantum gates may be quantified in a number of ways. Two of the most common metrics are the average gate fidelity, \mathcal{F} , and the diamond norm, $\|\cdot\|_\diamond$. These may be represented in terms of the error maps as

$$\|I - \mathcal{E}\|_\diamond = \sup_{\rho} \|(I \otimes I)(\rho) - (\mathcal{E} \otimes I)(\rho)\|_1 \quad (10)$$

$$\mathcal{F}(\mathcal{E}) = \frac{\text{Tr } \mathcal{E} + d}{d^2 + d} \quad (11)$$

Which metric is relevant depends on the application, and can yield very different numbers. For instance, the diamond norm is generally linear in the over-rotation angle of a quantum operation, while the average gate infidelity (AGI), given by $1 - \mathcal{F}$, is generally quadratic in the over-rotation angle of a quantum operation. These two metrics also vary significantly in performance on mixed processes.

A *mixed unitary process* (MUP) consists of a set of unitary channels, $\tilde{\mathcal{G}}_j$, and associated weights, $\sum_j \omega_j = 1$. The process matrix for a mixed unitary channel is then the weighted sum of the component channels, $\tilde{\mathcal{G}}_M = \sum_j \omega_j \tilde{\mathcal{G}}_j$, and the associated error channel is simply the weighted sum of the associated error channels, $\mathcal{E}_M = \sum_j \omega_j \mathcal{E}_j$. From this definition, we can use linearity to compute the AGI of a MUP. We see that the AGI of any MUP will be the convex sum of the constituent fidelities, with the same weighting. The diamond norm, however, is non-linear function of the channel, and can in general be smaller for a MUP than any of the processes being mixed.

Campbell[4] considered the important problem of minimizing the diamond norm of the resulting error channel. Given a collection of component channels with error at most ϵ , he showed that if the Hamiltonians form a convex set containing the origin, then the diamond norm can be quadratically suppressed. The diamond norm is a particularly appealing target because it provides useful error bounds on quantum circuits. However, it is not the only optimization target that can be chosen. If the ultimate goal is to produce a channel whose effect can be Monte Carlo simulated, then it may be useful instead to construct a channel whose errors are Pauli stochastic. Using a constrained numerical optimization routine, such a channel could be produced by minimizing the off-diagonal elements of R in Equation 3. Indeed, this is the approach we consider in our experimental implementation in Section V. More generally, as we will discuss, there are a number of options one may wish to consider when selecting weights to prepare a mixed unitary process.

III. CONSTRUCTING USEFUL UNITARY PROCESSES

A. A Simple Example

There are often many possible ways of implementing any given target quantum gate. Campbell and Hastings, for instance, consider gates compiled using the Solovay-Kitaev algorithm, for which many approximate gate compilations are possible.[4, 5] By selecting from these various implementations at random, they show that the resulting quantum channel can be made to have significantly reduced coherent error. As a simple example of how this occurs, consider a scenario in which we have a single-qubit and four possible implementations of a π -pulse about the σ_x axis. The error channels for these four implementations are themselves unitary rotations about the σ_x axis with rotation angles of $\{-2\epsilon, -\epsilon, \epsilon, 2\epsilon\}$. Such a situation could appear, for instance, if there were amplitude errors on the fields used to affect the gates, and if the control could be implemented by a rotation about the positive or negative σ_x axis.

Gate	H_{eff}	AGI	$\ \cdot\ _\diamond$
$\bar{U}_{+2\epsilon}$	$2\epsilon\sigma_x$	$4\epsilon^2$	2ϵ
$U_{+\epsilon}$	$\epsilon\sigma_x$	ϵ^2	ϵ
$U_{-\epsilon}$	$-\epsilon\sigma_x$	ϵ^2	ϵ
$U_{-2\epsilon}$	$-2\epsilon\sigma_x$	$4\epsilon^2$	2ϵ

In this case, the MUP that minimizes the diamond norm has matrix elements given by:

$$\frac{1}{2} \text{Tr}(\sigma_j^\dagger U_{-\epsilon} \sigma_k U_{-\epsilon}^\dagger) + \frac{1}{2} \text{Tr}(\sigma_j^\dagger U_{\epsilon} \sigma_k U_{\epsilon}^\dagger) \quad (12)$$

This channel will have a diamond norm proportional to ϵ^2 , whereas any other combination will have a nonzero linear dependence on ϵ . On the otherhand, any linear combination of $\{U_{\epsilon}, U_{-\epsilon}\}$ minimizes the AGI of the resulting channel with a value of ϵ^2 . Additionally, it is clear that it is favorable in both cases to draw from the channels with smaller error, rather than those with larger error, to minimize the multiplicative coefficient on the air. In [4] all channels are assumed to have performance less than some threshold, however in realistic scenarios some controls will have better performance than others, and it is important to select from those controls when able to.

Another interesting property of the MUP given in 12 is that it maintains its first-order insensitivity even in the presence of drift. If the control amplitudes that implement these gates drift, they will drift in equal and opposite ways. Thus the multiplicative prefactor on the diamond norm will vary in time, but the suppression of the first order insensitivity to the static detuning ϵ will be suppressed, as we will discuss later. Given these considerations from this simple example, the problem remains: given a collection of controls, how can one efficiently compute a weighting that minimizes a particular metric?

B. Diamond Norm Minimization

As discussed in [4], a sufficient condition to minimize the diamond norm of a MUP with error generators $\{H_j\}$ to first order is:

$$\sum \omega_j H_j = 0 \quad (13)$$

In [4] Campbell constructs an algorithm that, given an oracle to approximate unitaries, finds a MUP with this property. Alternatively, one can use convex optimization to solve this problem. Consider the matrix whose rows are the vectorized Hamiltonians at our disposal, i.e. for $m, n \times n$ Hamiltonians:

$$\mathbf{H} = \begin{pmatrix} H_{111} & H_{221} & \dots \\ \vdots & \ddots & \\ H_{m11} & & H_{mnn} \end{pmatrix} \quad (14)$$

If our weighting vector for our MUP is ω , we can rewrite this sum as a matrix product whose two-norm will be zero if and only if the sum is zero. Additionally, this optimization needs to be constrained so that ω only contains positive values that sum to one. Such a problem forms what is known as a convex optimization problem, and can be written with the following shorthand:

$$\text{minimize : } \|\mathbf{H}^T \omega\|_2 \quad \omega_j \geq 0, |\omega|_1 = 1 \quad (15)$$

where we write the constraints on the variable to be optimized over below the objective, and we write the cost function on the right. Linearly constrained minimizations with quadratic cost functions like this have been shown to be efficiently solvable by methods like the Ellipsoid Method, however these have very poor average case performance. Indeed, there are many existing convex solver software packages that solve these problems efficiently in practice, and formal proofs showing convergence in $\mathcal{O}(\log \frac{1}{\epsilon} L^2 n^4)$ time, where ϵ is the accuracy in the solution, L is the number of bits in the input, and n^4 is the number of variables.

C. Robustly Mixed Unitary Processes

While mixed unitary processes offer significant improvements to gate performance, they fail to take into account the reality that most control electronics experience drift over time scales relevant to QIP performance. Because of this drift, the quality of the MUP will degrade. Thus, we would like to design MUPs that are *robust* to this drift. To enforce robustness, we can consider higher derivatives of the Hamiltonians in 13. Instead of just requiring that the 0^{th} derivative averages to zero, we should impose a similar condition on the derivatives of the Hamiltonians with respect to parameters that may

drift:

$$D_j^n = \frac{1}{n!} \frac{\partial^n}{\partial \delta_{i_1} \dots \partial \delta_{i_n}} H_j(\vec{\delta})|_{\delta=\vec{0}} \quad (16)$$

If the dimension of $\vec{\delta}$ is d , the indices i_0, \dots, i_n take on values in $1, \dots, d$ and this matrix has d^n entries. We say that a mixed unitary process is said to be robust to order ℓ (an ℓ MUP) if for all $1 \leq k \leq \ell$:

$$\sum_j \omega_j \left(\sum_{n=0}^k D_j^n \right)^n = \vec{0} \quad (17)$$

In particular, we see that a 0MUP satisfies Equation 13. More generally, these conditions imply that an ℓ MUP is insensitive to the ℓ^{th} order in drift in $\vec{\delta}$. To see this, we can rewrite the error on each control in the MUP as:

$$\begin{aligned} \tilde{g}_j(\vec{\delta}) &= \exp(-i(H_j(\vec{0}) + \frac{\partial}{\partial \delta_i} H_j(d\delta_i) \\ &+ \frac{1}{2} \frac{\partial^2}{\partial \delta_i \partial \delta_k} H_j(d\delta_i d\delta_k) + \dots)) \mathcal{G} \end{aligned} \quad (18)$$

By Taylor expanding Equation 18 in $\vec{\delta}$, one finds that the the first ℓ derivatives of an ℓ MUP will be zero. Furthermore, if we are only interested in being first order insensitive to drift and can select controls such that $|D_j^n| \approx \epsilon$, we see that Equation 17 can be approximated as:

$$\sum_k \omega_j D_j^n = 0 \quad (19)$$

This condition guarantees that errors will be suppressed quadratically for all derivatives up to order ℓ . A proof is included in the appendix that generalizes the Hastings-Campbell Mixing Lemma in [4]. Namely, Campbell shows that if $0 \in \text{Conv}[\{H_i(\vec{\delta})\}]$, where Conv is the convex hull of its arguments, then an $\vec{\omega}$ exists that quadratically decreases the diamond norm. We prove that $0 \in \text{Conv}[\{D_j^n(\vec{\delta})\}]$ implies there is an $\vec{\omega}$ exists that quadratically decreases the ℓ^{th} -order sensitivity of the diamond norm of an ℓ MUP. Figure 2 gives geometric intuition for the conditions required to produce an ℓ MUP.

To generate robustly mixed unitary processes, we first define the vectorized derivative matrix D^ℓ in a similar way to 14:

$$\mathbf{D}^\ell = \begin{pmatrix} D_{111}^\ell & D_{221}^\ell & \dots \\ \vdots & \ddots & \\ D_{m11}^\ell & & D_{mnn}^\ell \end{pmatrix} \quad (20)$$

Using this, we can then solve the following convex optimization problem, generalizing Equation 15:

$$\begin{aligned} \text{minimize : } & \|\mathbf{D}^{\ell T} \omega\| \\ & \omega_j \geq 0, |\omega|_1 = 1 \\ \text{subject to : } & \forall n < \ell, \sum \omega_j D_j^n = \vec{0} \end{aligned} \quad (21)$$

with D_n^j defined in Equation 18. Note that these algorithms are independent of the number of rows, which in our case is the number of drifting parameters. However, the size of the matrix that must be computed grows as Nd^ℓ , and the runtime grows as N^4 , again with d being the number of drifting parameters, and N being the number of controls.

D. Hamiltonian Norm Regularization

While these particular convex optimization problem can be solved through a system of linear equations, casting it as a convex optimization problem allows us to regularize the cost function, and introduce additional constraints. In particular, while this minimization problem is sufficient for quadratically decreasing the diamond norm relative to the *worst* controls in the collection, it does not preferentially select the controls with the least error. That is to say, both $\{U_{+2\epsilon}, U_{-2\epsilon}\}$ and $\{U_\epsilon, U_{-\epsilon}\}$ from Section IIIB satisfy Equation 15. To encourage the inclusion of controls with smaller error, we may impose a penalty proportional to the norm of the included Hamiltonians. In our case, we chose to penalize for the ℓ_2 ($\|\cdot\|_2$) norm, and thus we modify our cost function to be:

$$\begin{aligned} & \text{minimize}_{n \in [N]} \{ \\ & \quad \text{minimize} : \|\mathbf{D}^{\ell^T} \omega\| + \eta \sum \omega_j \|D_j^0\|_2 \\ & \quad \omega_j \geq 0, |\omega|_1 = 1 \\ & \quad \text{subject to: } \forall n < \ell, \sum \omega_j D_j^n = 0 \\ & \} \end{aligned} \quad (22)$$

with $\eta \geq 0$. By making η larger, we can suppress the diamond norm to second order, while ensuring that we are selecting those that will give us a smaller prefactor.

E. Sparsity Constraints

As a practical consideration, we would also like to regularize our objective function to enforce sparsity. Control electronics often have a limited amount of waveform memory, and thus it is important that MUPs have non-trivial probability support on a small number of controls. As an example of where this would be necessary is Figure 2. In Subfigure b, it's clear that H_4 is unnecessary to contain the origin in the convex hull of the error generators. However, if we additionally want our controls to form a 1MUP, we see from Subfigure D that we need H_4 in our control set. Thus we would like the solver to be frugal in which controls it selects. In many machine learning situation, lasso regularization [8] can be used to enforce sparsity, however here it is insufficient as we already constrain the one norm of the vector we optimize over to be one. Conveniently, the problem of enforcing

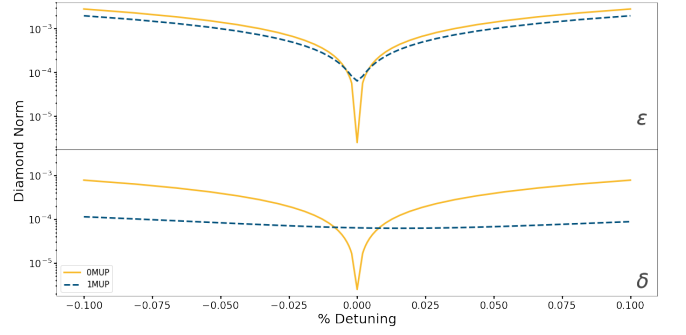


FIG. 3. Numerical results comparing a 0MUP to a 1MUP for a single tunable qubit, for $RY(\frac{\pi}{2})$. The results are qualitatively similar to those for $RX(\frac{\pi}{2})$. In this case the 0MUP outperforms both the 1MUP by two orders of magnitude, and the constituent controls by three orders of magnitude at the origin. However, varying over δ we see that the 1MUP outperforms the 0MUP by up to an order of magnitude when there is .1% drift in the qubit control amplitudes.

sparsity in such situations has been considered in [9] and can be expressed via another convex program that extends Equation 15:

$$\begin{aligned} & \text{minimize}_{n \in [N]} \{ \\ & \quad \text{minimize} : \|\mathbf{D}^{\ell^T} \omega\| + t \\ & \quad \omega_j \geq 0, |\omega|_1 = 1, \\ & \quad t \geq 0 \\ & \quad \text{subject to: } \omega_n > \frac{\lambda}{t} \\ & \quad \quad \forall n < \ell, \sum \omega_j D_j^n = 0 \\ & \} \end{aligned} \quad (23)$$

where λ is a hyperparameter to be optimized over.

IV. NUMERICAL RESULTS

In the following numerical results, we explore using the methods in Section III to build MUPs. We consider the following model for a single tunable qubit:

$$H(\delta, \epsilon, t) = \epsilon \sigma_z + (1 + \delta)(c_x(t)\sigma_x + c_y(t)\sigma_y) \quad (24)$$

We use the GRAPE algorithm as discussed in Section ?? with $N=25$ steps and total evolution time of π to generate 100 candidate controls, with a standard deviation of $\sigma = .001$ for the distribution in Equation ?. We assume that the errors on σ_x and σ_y are perfectly correlated, as is the case in systems that implement RZ rotations with phase shifts of the control signal. Solving the optimization problem defined in Section IIIC yields similar MUPs for $RX(\frac{\pi}{2})$ and $RY(\frac{\pi}{2})$, with the results for $RY(\frac{\pi}{2})$ shown in Figure 3. These results demonstrate several properties that make MUPs both useful and tractable.

First, naively generating a 0MUP results in nontrivial support on all the members of the control family. However, by rewriting the minimization to impose the sparsity constraint discussed in Section III C, we can generate a 0MUP that uses just five of the controls. This shows that through adding constraints to our optimization routine, we can make the MUP practically useful. In both cases we impose the same ℓ_2 penalty as described in Section III C, so that the algorithm preferentially selects controls with smaller errors. Imposing this constraint allows us to trade off flatness at the origin for performance.

A. Two Qubit Performance Analysis

In our two-qubit example we consider the following model for two tunable qubits coupled by a resonant exchange interaction, similar to that in [15]:

$$H(\vec{\delta}, \vec{\epsilon}, t) = \sum_{j=1}^2 (\epsilon_j \sigma_z^j + (1 + \delta_j)(c_x^j x(t) \sigma_x^j + c_y^j(t) \sigma_y^j)) + \frac{1}{10}(XX + YY) \quad (25)$$

In this example it was infeasible to use GRAPE to return non-trivial solutions. Instead we manually selected piecewise constant echoing sequences with 500 steps and total evolution time of $\frac{5\pi}{2}$. In particular, we considered $RX(\pi)$, $RX(-\pi)$, $RY(\pi)$ and $RY(-\pi)$ bang-bang sequences [16], consisting of all combinations of simultaneous π pulses activated at multiples of 8 steps from the beginning of the controls, and the same multiple of 8 steps prior to the end of the controls. To give the control family a variety of RF errors, we added on uniformly distributed errors to each π pulse, between -0.25% and 0.25% .

In this example, we find more modest improvements to performance, as shown in Figure 4. There are now four free parameters to optimize over, and the uncontrolled entangling interaction means that there is little room for variation in the controls. Nonetheless, using a MUP improves performance by half of an order of magnitude at the origin relative to the constituent controls, and up to an order of magnitude away from the origin. For all values of the drifting parameters we see that the 1MUP performs as well or better than 0MUP.

V. EXPERIMENTAL RESULTS

Here we present experimental results from implementing our routine on a fixed-frequency superconducting transmon qubit. In particular, we used qubit 8 on the Rigetti 19Q-Acorn chip, whose characterization can be found in [17]. To implement a MUP on this qubit, four incorrectly calibrated Gaussian pulses were produced by

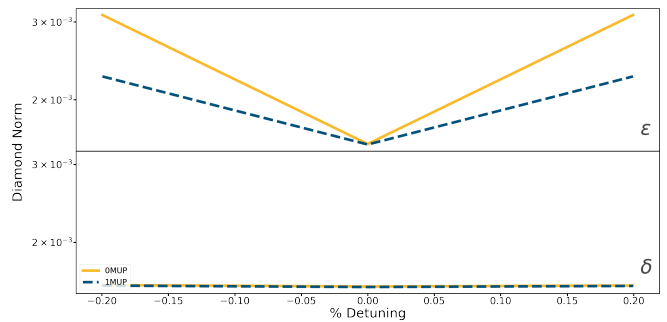


FIG. 4. Numerical results comparing a 0MUP to a 1MUP for a pair of tunable qubits, with a resonant exchange interaction. Shown with lower alpha values are example constituent controls. The 0MUP and 1MUP can be seen to outperform these controls by half of an order of magnitude at the origin. For all detuning values the 1MUP performs as well or better than the 0MUP. When there is 0.2% drift in the qubit frequency, the 1MUP outperforms members of the control families by almost an order of magnitude in diamond norm. Similarly, for 0.2% drift in the qubit control amplitude, we see that the 1MUP outperforms the constituent controls by over half an order of magnitude.

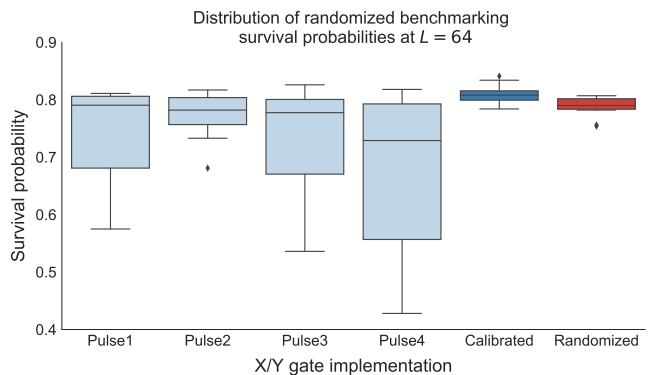


FIG. 5. Randomized benchmarking experiments ran using different pulse definitions. The four plots on the left are from the incorrectly calibrated pulse, while the top right is the calibrated pulse, and the bottom right is the MUP.

scaling the pulseshape amplitude for a calibrated 10 sample 50ns $RX(\frac{\pi}{2})$ pulse by 106.4%, 103.9%, 93.7% and 91.2%.

As discussed in Section III C, we chose here to minimize the off diagonal elements of the process matrix. To benchmark the quality of the MUP, we then performed six randomized benchmarking experiments[18]: one for each over- and under-calibrated pulse, one for the calibrated pulse, and one for the mixed process. We used 1000 shots per experiment, 10 sequences per sequence length, for sequence lengths of 2, 4, 8, 16, 32 and 64. In each case, our Clifford operations were decomposed into $RX(\frac{\pi}{2})$ and $RY(\frac{\pi}{2})$ pulses. In our implementation, these gates are implemented using the same pulse envelope definitions and control electronics, phase shifted

by $\frac{\pi}{2}$ radians, and are therefore subject to identical miscalibration errors. The results are shown in Figure 5 for sequence lengths $L = 64$. Fitting to the randomized benchmarking decay curves, we find one-qubit gate fidelities of 99.3% for the calibrated pulse, 98.9% for Pulse1, 99.1% for Pulse2, 98.9% for Pulse3, 98.5% for Pulse4, and 99.2% for the MUP, demonstrating that it performs almost as well as the calibrated pulse, and better than the constituent pulses.

Additionally, by minimizing the off-diagonal elements of the process matrix, rather than balancing the Hamiltonian errors, we expect to produce a process with minimal coherent error in the absence of drift. To see that this is the case, we cite the results in [19]. For non-Markovian error models, noise will manifest as gamma distributed points for each sequence length. On the other hand, Markovian noise, such as depolarizing noise, will result in Gaussian distributed fidelity estimates for each randomized benchmarking sequence length. We see that the coherently miscalibrated controls in our RB experiment have long tails, consistent with gamma distributed random variables, while the calibrated and randomized implementations both have much shorter tails, consistent with Gaussian distributed random variables. Thus, our experiment demonstrates that not only is the performance of the MUP better than the constituent gates, it also has a significantly less-coherent error channel.

VI. CONCLUSION AND FUTURE WORK

We have shown numerically that using MUPs can reduce coherent error on a quantum channel by more than an order of magnitude in diamond norm, over a wide range of quasi-static values of noise. In addition, we have demonstrated that these approximate controls can be generated through optimal control (GRAPE), and that the minimization problem is tractable.

Future directions for this work include demonstrating the routine experimentally on a two-qubit gate, moving the random gate selection from a precompilation step to runtime logic onboard the control electronics, investigating other optimization routines such as CRAB [11] and GOAT[12], and using more sophisticated benchmarking routines such as GST[20] to quantitatively investigate the performance of our method.

Another interesting area of research would be using model-free approaches. The numerical work in the paper assumes access to a model of the system, however an experimentalist may not have a model readily available to describe the system, e.g. in the presence of unknown on-chip crosstalk, or an uncalibrated transfer function of the system. Even if a model is available, it might be computationally inconvenient to simulate, i.e. for more than a few qubits.

In these situations, one approach would be to use *in-situ* optimal control techniques [21–23] to generate candidate controls, and then use an optimizer like Nelder-Mead to perform the minimization. While performing a complete optimization in this way would require full process tomography, one could instead optimize via partial tomography. By selecting pre- and post-rotations that correspond to measuring Pauli-moments of interest in the Hamiltonian, such as unwanted $Z \otimes Z$ crosstalk, one could perform optimization over fewer parameters.

VII. ACKNOWLEDGEMENTS

Sandia National Laboratories is a multimission laboratory managed and operated by National Technology and Engineering Solutions of Sandia, LLC, a wholly owned subsidiary of Honeywell International, Inc., for the U.S. Department of Energy’s National Nuclear Security Administration under contract DE-NA0003525.

-
- [1] R. Barends, J. Kelly, A. Megrant, A. Veitia, D. Sank, E. Jeffrey, T. C. White, J. Mutus, A. G. Fowler, B. Campbell, Y. Chen, Z. Chen, B. Chiaro, A. Dunsworth, C. Neill, P. O’Malley, P. Roushan, A. Vainsencher, J. Wenner, A. N. Korotkov, A. N. Cleland, and J. M. Martinis, *Nature* **508**, 500 (2014).
 - [2] C. Ballance, T. Harty, N. Linke, M. Sepiol, and D. Lucas, *Physical Review Letters* **117** (2016), 10.1103/physrevlett.117.060504.
 - [3] J. Preskill, “Quantum computing and the entanglement frontier,” (2012), [arXiv:1203.5813](#).
 - [4] E. Campbell, *Physical Review A* **95** (2017), 10.1103/physreva.95.042306.
 - [5] M. B. Hastings, “Turning gate synthesis errors into incoherent errors,” (2016), [arXiv:1612.01011](#).
 - [6] E. Campbell, “A random compiler for fast hamiltonian simulation,” (2018), [arXiv:1811.08017](#).
 - [7] K. Rudinger, T. Proctor, D. Langharst, M. Sarovar, K. Young, and R. Blume-Kohout, “Probing context-dependent errors in quantum processors,” (2018), [arXiv:1810.05651](#).
 - [8] R. Tibshirani, *Journal of the Royal Statistical Society. Series B (Methodological)*, 267 (1996).
 - [9] M. Pilanci, L. E. Ghaoui, and V. Chandrasekaran, in *Advances in Neural Information Processing Systems 25*, edited by F. Pereira, C. J. C. Burges, L. Bottou, and K. Q. Weinberger (Curran Associates, Inc., 2012) pp. 2420–2428.
 - [10] N. Khaneja, T. Reiss, C. Kehlet, T. Schulte-Herbrüggen, and S. J. Glaser, *Journal of Magnetic Resonance* **172**, 296 (2005).
 - [11] T. Caneva, T. Calarco, and S. Montangero, *Physical Review A* **84** (2011), 10.1103/physreva.84.022326.
 - [12] S. Machnes, E. Assémat, D. Tannor, and F. K. Wilhelm, *Physical Review Letters* **120** (2018), 10.1103/phys-

- revlett.120.150401.
- [13] M. H. Goerz, E. J. Halperin, J. M. Aytac, C. P. Koch, and K. B. Whaley, *Physical Review A* **90** (2014), 10.1103/physreva.90.032329.
 - [14] M. Abramowitz and I. Stegun, National Bureau of Standards, US Government Printing Office, Washington, DC (1972).
 - [15] D. C. McKay, S. Filipp, A. Mezzacapo, E. Magesan, J. M. Chow, and J. M. Gambetta, *Physical Review Applied* **6** (2016), 10.1103/physrevapplied.6.064007.
 - [16] L. Viola and S. Lloyd, *Physical Review A* **58**, 2733 (1998).
 - [17] J. S. Otterbach, R. Manenti, N. Alidoust, A. Bestwick, M. Block, B. Bloom, S. Caldwell, N. Didier, E. S. Fried, S. Hong, P. Karalekas, C. B. Osborn, A. Papageorge, E. C. Peterson, G. Prawiroatmodjo, N. Rubin, C. A. Ryan, D. Scarabelli, M. Scheer, E. A. Sete, P. Sivarajah, R. S. Smith, A. Staley, N. Tezak, W. J. Zeng, A. Hudson, B. R. Johnson, M. Reagor, M. P. da Silva, and C. Rigetti, “Unsupervised machine learning on a hybrid quantum computer,” (2017), arXiv:1712.05771.
 - [18] E. Magesan, J. M. Gambetta, and J. Emerson, *Physical Review Letters* **106** (2011), 10.1103/physrevlett.106.180504.
 - [19] H. Ball, T. M. Stace, S. T. Flammia, and M. J. Biercuk, *Physical Review A* **93** (2016), 10.1103/physreva.93.022303.
 - [20] R. Blume-Kohout, J. K. Gamble, E. Nielsen, K. Rudinger, J. Mizrahi, K. Fortier, and P. Maunz, *Nature Communications* **8** (2017), 10.1038/ncomms14485.
 - [21] R.-B. Wu, B. Chu, D. H. Owens, and H. Rabitz, *Physical Review A* **97** (2018), 10.1103/physreva.97.042122.
 - [22] J. Kelly, R. Barends, B. Campbell, Y. Chen, Z. Chen, B. Chiaro, A. Dunsworth, A. Fowler, I.-C. Hoi, E. Jeffrey, A. Megrant, J. Mutus, C. Neill, P. O’Malley, C. Quintana, P. Roushan, D. Sank, A. Vainsencher, J. Wenner, T. White, A. Cleland, and J. M. Martinis, *Physical Review Letters* **112** (2014), 10.1103/physrevlett.112.240504.
 - [23] C. Ferrie and O. Moussa, *Physical Review A* **91** (2015), 10.1103/physreva.91.052306.

VIII. APPENDIX

A. Robust Mixing Lemma

We begin by generalizing Lemma 2 from [4]. If all of our error Hamiltonians $\{H_j\}$ have bounded error, that is:

$$\|H_j\| \leq c \quad (26)$$

Then we may consider the derivative of any mixture of unitaries as:

$$\frac{d}{d\delta} \sum_j \omega_j e^{iH_j} = \sum_j \omega_j i \frac{d}{d\delta} (H_j) e^{iH_j} \quad (27)$$

By assumption, the derivatives of the first order term sum to zero, and so we see by A3 in [4] that

$$\left\| \frac{d}{d\delta} \sum_j \omega_j e^{iH_j} \right\| \leq \sum_j \omega_j \left\| i \frac{d}{d\delta} (H_j) (iH_j + \sum_{n=2}^{\infty} \frac{(iH_j)^n}{n!}) \right\| \leq \sum_j \omega_j (c^2 + \frac{c^2}{2}) \leq c^2 + \frac{c^3}{2} \quad (28)$$

Where we have used the fact that $\|AB\| \leq \|A\| \|B\|$ with $\|\cdot\|$ being the ∞ -norm. Additionally,

$$\left\| \frac{d}{d\delta} e^{iH_j} \right\| = \left\| \frac{d}{d\delta} (iH_j) e^{iH_j} \right\| \quad (29)$$

$$\leq \left\| \frac{d}{d\delta} (iH_j) \right\| + \left\| \frac{d}{d\delta} (iH_j) H_j \right\| + \left\| \frac{d}{d\delta} (iH_j) \sum_{n=2}^{\infty} \frac{1}{(n)!} (iH_j)^n \right\| \quad (30)$$

$$\leq \left\| \frac{d}{d\delta} (iH_j) \right\| + \left\| \frac{d}{d\delta} (iH_j) \right\| \cdot \|H_j\| + \left\| \frac{d}{d\delta} (iH_j) \right\| \cdot \left\| \sum_{n=2}^{\infty} \frac{1}{(n)!} (iH_j)^n \right\| \quad (31)$$

$$\leq c + c^2 + \frac{c^3}{2} \quad (32)$$

And so we see that Lemma 2 generalizes. We will use the above to upper bound the 1-norm (and hence diamond norm) in the following.

Next we generalize the Mixing Lemma from [4]. We must assume that the 1-norm is uniformly differentiable. In that case, we see that:

$$= \frac{d}{d\vec{\delta}} \sup |\mathcal{I} \otimes \mathcal{I} - \mathcal{E}(\vec{\delta}) \otimes \mathcal{I}|_1 \quad (33)$$

$$= \sup \frac{d}{d\vec{\delta}} |\mathcal{I} \otimes \mathcal{I} - \mathcal{E}(\vec{\delta}) \otimes \mathcal{I}|_1 \quad (34)$$

$$\leq \sup \left| \frac{d}{d\vec{\delta}} (\mathcal{I} \otimes \mathcal{I} - \mathcal{E}(\vec{\delta}) \otimes \mathcal{I}) \right|_1 \quad (35)$$

$$(36)$$

And so we see it is sufficient to upperbound:

$$\left| \frac{d}{d\vec{\delta}} (\mathcal{I} \otimes \mathcal{I} - \mathcal{E}(\vec{\delta}) \otimes \mathcal{I}) \right|_1 \quad (37)$$

From Equation 18 in [4]:

$$(\mathcal{V} \circ \mathcal{E} - \mathbb{1})(X) = \sum_j \omega_j (\tilde{\delta}_j X + X \tilde{\delta}_j^\dagger + \tilde{\delta}_j X \tilde{\delta}_j^\dagger) \quad (38)$$

$$\frac{d}{d\vec{\delta}} (\mathcal{V} \circ \mathcal{E} - \mathbb{1})(X) = \sum_j \omega_j \left(\frac{d}{d\vec{\delta}} \tilde{\delta}_j X + X \frac{d}{d\vec{\delta}} \tilde{\delta}_j^\dagger + \frac{d}{d\vec{\delta}} \tilde{\delta}_j X \tilde{\delta}_j^\dagger + \tilde{\delta}_j X \frac{d}{d\vec{\delta}} \tilde{\delta}_j^\dagger \right) \quad (39)$$

$$(40)$$

Thus, by Hölder's inequality we find:

$$\left\| \frac{d}{d\vec{\delta}} (\mathcal{V} \circ \mathcal{E} - \mathbb{1})(X) \right\|_1 \leq \left\| \sum_j \omega_j \frac{d}{d\vec{\delta}} \tilde{\delta}_j \right\| + \left\| \sum_j \omega_j \frac{d}{d\vec{\delta}} \tilde{\delta}_j^\dagger \right\| + \sum_j \omega_j \left\| \frac{d}{d\vec{\delta}} \tilde{\delta}_j \right\| \cdot \left\| \tilde{\delta}_j^\dagger \right\| + \sum_j \omega_j \left\| \tilde{\delta}_j \right\| \cdot \left\| \frac{d}{d\vec{\delta}} \tilde{\delta}_j^\dagger \right\| \quad (41)$$

By assumption, all of these terms are negligible, and therefore we find:

$$\left\| \frac{d}{d\vec{\delta}} (\mathcal{V} \circ \mathcal{E} - \mathbb{1})(X) \right\|_1 \leq 2a^2 + 2b^2 \quad (42)$$

And so we see that the mixing lemma extends to first order. In a similar way, it can be extended to arbitrary order, and thus if we can find constructions that satisfy the generalized Lemma 2, we can use the Robust Mixing Lemma to conclude that there exists a weighting with linearly suppressed diamond norm.